An Initial Analysis of the Stationkeeping Tradespace for Constellations

Andris Slavinskis
Bay Area Environmental Research Institute
NASA Ames Research Center
Moffett Field, Mountain View, CA 94035

Tartu Observatory, University of Tartu
Observatooriumi 1, Tõravere
61602 Tartu county, Estonia
Mobile: +372 58284333
andris.slavinskis@ut.ee

Sreeja Nag
Bay Area Environmental Research Institute
NASA Goddard Space Flight Center
8800 Greenbelt Rd, Greenbelt, MD 20771
sreeja.nag@nasa.gov

Joel Mueting
Metis Technology Solutions
NASA Ames Research Center
Moffett Field, Mountain View, CA 94035
joel.r.mueting@nasa.gov

Abstract—**This paper presents an Orbit Maintenance Module (OMM) for Tradespace Analysis Tool for Constellations (TAT-C), a software package to explore a wide range of tradespaces to design constellations for Earth observation. As the tool is primarily meant for rapid pre-Phase A analysis, it has to be able to estimate trade-offs and overall performance parameters with simplified models on a personal computer in a reasonable time frame. The OMM estimates the secular drift of relative orbital elements between pairs of satellites due to the gravitational 'J2' effects and the drift of altitude due to the atmospheric drag, and computes maneuvers to correct them. The J2 is a predominant term in the gravitational zonal harmonics which, primarily, affects the argument of perigee and the mean anomaly. We estimate the drift of these elements between pairs of satellites using a fourth-order polynomial, which is trained using machine learning and which depends on the inclination, altitude and initial angular separation in true anomaly and right ascension of the ascending node. An analytical model is used to predict the deorbiting rate depending on the initial altitude, the solar cycle, the satellite's mass, drag coefficient and area. In order to maintain the required topology of a constellation, the drift of orbital elements is compensated using emulated orbital maneuvers, when satellites breach a user-defined threshold percentage of their nominal values. We assume simple orbital maneuvers (i.e., orbit phasing and Hohmann transfer) to determine the required delta-V, propellant consumption and frequency of maneuvers. These parameters are provided as outputs of the TAT-C's OMM, which advises the user on trade-offs between performance and maintenance overhead of all enumerated constellation architectures. The maneuver metrics can be used to determine various dependent metrics, such as time available for observations, impact on total satellite mass, and mission cost.**

978-1-5386-6854-2/19/$31.00

Table of Contents

1. Introduction

In the recent decade, constellations of Earth observation satellites are gaining momentum with many mission designs and a few operational missions. Exciting advancements have been made in the use of multiple satellites to improve the revisit time and/or to diversify the measurement type. For example, the Afternoon Constellation (A-Train) had seven satellites in a train formation launched between 2002 and 2014, each taking different measurements to characterize the environment. Planet Labs Inc. is imaging every location of the Earth every day with a flock of more than 200 satellites. While Planet's CubeSats are distributed in orbit using the differential drag, constellations of larger and more advanced satellites, such as Iceye, will need to maintain a certain topology to maximize the output of each satellite.

In addition to the complexity of conventional mechanics of single satellites, the constellation design poses new challenges associated with an increased number of satellites and their topology. In order to address these and other challenges related to the constellation design, Tradespace Analysis Tool for Constellations (TAT-C) is being developed by NASA Goddard Space Flight Center and collaborators. TAT-C facilitates pre-Phase A investigations and optimizes Earth Observation (EO) constellations with respect to *a priori* science goals. It helps to choose the type of a constellation, number of satellites, and what trade-offs are associated with various designs. [1], [2]

This paper presents the TAT-C's Orbit Maintenance Module (OMM) which estimates the relative secular drift in orbital elements, and the trade-offs associated with corresponding orbital maneuvers. We characterize relative drifts due to two dominating effects – the Earth's oblateness and the atmospheric drag. By accounting for these effects, we can derive the first-order estimation of the ΔV budget for maintaining the constellation's topology. Typically, such analyses are performed by numerically propagating orbits with perturbations. However, it is not possible to run full-fledged or even limited orbit propagators for a range of inclinations, altitudes, orbital planes, angular separations between satellites and for a number of satellites in a reasonable time frame.

The Earth's gravitational potential can be expressed using spherical harmonics with coefficients J_n [3]. The J_2-term expresses the effect of the Earth's North–South hemisphere oblateness which is larger than other terms by orders of magnitude and, therefore, dominates the gravitational perturbations. The mean classical orbital elements can be used to calculate the absolute secular drift of the Right Ascension of the Ascending Node (RAAN), the Argument Of Perigee (AOP) and the Mean Anomaly (MA). To the first order of J_2, there are no long-periodic and no secular variations in the remaining orbital elements [4, p. 37] [5, p. 647–652]. The mean elements are invariant with respect to the True Anomaly (TA) or the MA which means that the predicted drift will be equal for satellites with the same Semi-Major Axis (SMA), inclination and eccentricity. However, two satellites with different TAs in the same orbit experience slightly different gravitational potential which introduces a relative drift in their angular separation.

The atmospheric drag causes orbital decay – a decrease in the SMA which, in turn, causes the orbital period to decrease and the velocity to increase. For a circular orbit, these changes can be modeled depending on the drag coefficient, the drag area, the satellite's mass and the atmospheric density [6, p. 215]. While the first three depend on the satellite design and are generally known by engineers, the atmospheric density depends on various factors, such as effects of the day–night, semi-annual and 11-year solar-cycle variations in the air density. For EO mission analyses in TAT-C, the lifetime is typically much larger than one year and the altitude is larger than 300 km. Therefore, the most profound changes in the atmospheric density are induced by solar cycles. We are interested in designing future missions but predicting the solar activity is a rather difficult task. We use a very rough-and-ready method to calculate the atmospheric density depending on the density estimation during the solar minimum and the maximum, as well as the time within a solar cycle. [7, p. 241–251]

The OMM is designed to explore the following tradespaces in homogenous constellations, with satellites distributed uniformly according to the Walker pattern or with user-defined initial elements.

- Altitude between 300 and 1000 km;
- Inclination between 0° and 180°;
- TA between 0° and 360°;
- RAAN between 0° and 360°;
- Number of satellites between 2 and 72;
- Number of orbital planes between 1 and 72.

TAT-C can also explore the tradespace of heterogeneous Walker and ad-hoc constellations, as well as precessing-type and train constellations [8]. The first two are not designed to be maintained in a constant topology, however if certain aspects of their topology (e.g., the spread of satellites in a single orbital plane) are required to be preserved, some models presented here can be applied. Maintenance of the last two can be computed in the same way as homogeneous Walker, once deployment is complete and orbits are stable, therefore all the results of this paper will hold for them as well.

To estimate the secular drift of the angular separation due to J_2, we use General Mission Analysis Tool (GMAT) to run a large number of Monte Carlo simulations in the given Keplerian element ranges for five days. Results show that data from longer simulations lead to higher fidelity results for multi-plane constellations, however, the proposed methodology remains the same. Each simulated constellation consists of 72 satellites which maximizes the number of pairs. By analyzing the drift between non-neighbors, we can effectively study a smaller constellation. The implementation presented in this paper assumes that at a given altitude and inclination, secular relative drift rates are linear and, therefore, can be scaled for other time frames. Orbits are near circular with an eccentricity of 0.001 which also makes the TA and the MA numerically very similar.

The drift rate of the AOP alone is of a little interest. However, since the perigee serves as a reference for TA and MA, the relative drift in the Argument Of Latitude (AOL), a sum of AOP and TA, is used to measure the drift between satellites within orbit. The benefit of using the AOL is its stable reference – the ascending node. Furthermore, the relative AOL is also used as the phase difference between satellites in adjacent planes.

The investigation of the relative RAAN drift showed negligible rates – at an order of magnitude of one degree per year between satellites with different RAANs and even less for satellites with equal initial RAANs. In addition, RAAN maneuvers require ΔV-expensive plain changes which have to be carefully considered when designing a mission. Therefore, for the purpose of OMM's rapid pre-Phase A analysis, relative RAAN drift rates are not considered.

For the AOL, we find the largest relative drift rates depending on the altitude, inclination, as well as initial TA and RAAN separations. Although the absolute initial TA influences the relative AOL drift rate, the model is trained to estimate the maximum values because specific TAs are not known before the Phase A. The initial altitude, inclination and TA/RAAN separations along with largest drift rates after five days are used to train polynomial regression models with machine learning. We train a fourth-order model at seven inclination groups between 6° and 174°. For equatorial orbits (inclinations in the range of 6°), we train a liner model that depends on the initial TA separation and the altitude. As a result, we have a model that predicts the maximum relative drift rate in the AOL in nine inclination groups depending on the initial conditions and the time frame. To account for various drift rates depending on the initial TA when emulating a constellation, the drift rates are scaled using a cosine. The models are verified and characterized using a data set from independent simulations.

Since the AOL drift model depends on the altitude, it is coupled with a deorbiting model which predicts the change in altitude due to the atmospheric drag. In order to estimate the ΔV budget, the timeline of maneuvers and the propellant consumption, drift-prediction models are run iteratively until satellites breach a user-defined threshold percentage of their nominal values, or the end of mission lifetime is reached. When a correction is required, the OMM calculates maneuver metrics by assuming either orbit phasing or Hohmann transfer maneuvers to correct for the AOL drift or altitude drop, respectively. After emulating a maneuver, a relative orbital element is set to its nominal value.

The paper is organized as follows. Section 2 presents development and validation of models that estimate the AOL relative drift rate due to J_2. Section 3 presents the model that estimates the altitude drop due the atmospheric drag along with validation of the model. Section 4 presents the coupling of models, algorithm for orbit maintenance, and validation with GMAT which simulates perturbations along with actual maneuvers.

2. Gravitational perturbations

Drift estimation model

Gravitational perturbations cause two satellites to drift with respect to each other. Here we present a model to estimate the relative drift exptected in the AOL. To estimate largest drift rates, a general model, given by Equation 1, is used [9].

$$h = \theta_0 x_0 + \theta_1 x_1 + \ldots + \theta_n x_n \qquad (1)$$

h is the hypothesis that correspond to target variables (see y_M below).

$\theta_{0\ldots n}$ are coefficients, expressed as Θ in a vector form.

$x_{0\ldots n}$ are features.

When training the model, we must find Θ via the normal equation (Formula 2) where X, given by Equation 3, is defined by numerical values of features of all training samples.

$$\Theta = (X^T X)^{-1} X^T y_M \qquad (2)$$

$$X = \begin{pmatrix} x_0(1) & x_1(1) & \cdots & x_n(1) \\ x_0(2) & x_1(2) & \cdots & x_n(2) \\ \vdots & \vdots & \ddots & \vdots \\ x_0(m) & x_1(m) & \cdots & x_n(m) \end{pmatrix} \qquad (3)$$

m is the number of training samples.

Θ must be be solved for AOL drift rates in nine inclination groups, as detailed below. $\Theta(i)$ is used to distinguish coefficients for different inclination groups.

y_M is a vector of target variables of relative AOL drift rates in their worst cases (i.e., maximum drift rates at certain initial conditions).

When applying the model, we must solve Equation 4. If the model is used to predict a single case, X is a vector.

$$y_M = \Theta X \qquad (4)$$

The following considerations are used when selecting features. These consideration steam from the initial attempt to develop a linear model which proved to be insufficient and, therefore, is not presented in the paper.

- To estimate the maximum AOL drift rates, at least a fourth-order polynomial is needed because the behavior is not always symmetric with respect to the 90° initial TA separation as a parabola would imply, and cubic function's two bends would also not suffice.
- The inclination, the altitude and the initial RAAN separation seem to be correlated with the initial AOL separation. Therefore, we use all of them to define the initial conditions for estimating maximum drift rates.
- Drift rates at equatorial orbits are difficult to predict (i.e., characterize with a certain function). A linear function is used to set an upper threshold (somewhat similar as assigning a rectangular probability distribution for measurements with an unknown distribution).

We found the features defined by Equation 5 to be useful at predicting the maximum relative drift in most of the cases.

$$\begin{array}{llll} x_0 = 1 & x_1 = \nu_s & x_2 = \nu_s^2 & x_3 = \Omega_s \\ x_4 = \Omega_s^2 & x_5 = i & x_6 = i^2 & x_7 = z \\ x_8 = \nu_s \Omega_s & x_9 = \nu_s^2 \Omega_s & x_{10} = \nu_s \Omega_s^2 & x_{11} = \nu_s^2 \Omega_s^2 \\ x_{12} = \nu_s i & x_{13} = \nu_s^2 i & x_{14} = \nu_s i^2 & x_{15} = \nu_s^2 i^2 \\ x_{16} = \nu_s z & x_{17} = \nu_s^2 z & x_{18} = \nu_s^3 & x_{19} = \nu_s^4 \end{array} \qquad (5)$$

ν_s is the initial TA separation in the range [0°, 180°].

Ω_s is the initial RAAN separation in the range [0°, 180°].

z is the altitude in the range [300 km, 1000 km].

i is the inclination in the range [0°, 90°]. If the inclination is in the range [90°, 180°], then $i_{sym} = 180° - i$ should be used.

The solution (i.e., specific Θ) is sensitive with respect to the inclination. In other words, a single Θ is not efficient at predicting drift rates at various inclinations (at least with our model). Therefore, we use the following inclination groups to train and use the model:

- 6°–20° & 160°–174°;
- 20°–40° & 140°–160°;
- 40°–55° & 125°–140°;
- 55°–70° & 110°–125°;
- 70°–85° & 95°–110°;
- 85°–90°;
- 90°–95°;
- 0°–6°;
- 174°–180°.

Note that the inclination itself is not affected by the J_2 and drag, which allows us to keep the inclination group as a constant in the simulation throughout the mission lifetime. Moreover, the last two (equatorial) groups are trained with a set of just two features defined by Equation 6.

$$x_0 = 1 \quad x_1 = \nu_s z \tag{6}$$

Application of model on any constellation architecture

As noted earlier, y_M is an estimate of the maximum drift rate at certain initial conditions. Within a constellation, drift rates vary from satellite to satellite between $\pm y_M$. Therefore, within an orbital plane, values are adjusted using a cosine. Since the model was trained for a period of five days (432000 seconds), linear scaling of drift rates is required when different periods are considered. We emulate a constellation in terms of y_s (per Equation 7) and y_p (per Equation 8), as described below.

$$y_s = \frac{t y_M}{432000} cos\left(\frac{\pi((s + r_s) \bmod N_s)}{N_s}\right) \tag{7}$$

y_s is the relative AOL drift rate of the s^{th} satellite pair in an orbital plane.

s is the pair's index in the range [1, N_s].

N_s is the number of pairs per plane.

r_s is an integer in the range [1, N_s]. r_1 is selected randomly and increased by one when drift rates for the pair $s + 1$ are calculated. The expression $(s + r_s) \bmod N_s$ randomizes at which satellite the periodic function starts when initiating a constellation. Without such randomization, the first and the last satellite within an orbital plane would always be assigned largest $\pm y_M$ values which is not realistic.

t is the period for which drift rates are estimated.

Similar behavior is assumed for drift rates between satellites in different orbital planes. However, as explained in Section 4, the inter-plane AOL drift is not necessarily linear. The inter-plane relationship is expressed in Equation 8. We assume that all satellites within a plane have this same relative drift with respect to all satellites in another plane.

$$y_p = \frac{t y_M}{432000} cos\left(\frac{2\pi((p + r_p) \bmod N_p)}{N_p}\right) \tag{8}$$

y_p is the relative AOL drift rate between satellites in the p^{th} orbital plane pair. When calculating y_M, note that $\nu_s = \frac{360°}{N_s N_p}$, according to the Walker-Delta pattern.

p is the index of an orbital plain pair in the range [1, N_p].

N_p is the number of orbital planes.

r_p is an integer in the range [1, N_p] with a similar function and behavior as r_s.

Note that Equations 7 and 8 merely give a rough approximation how the relative AOL drift rate vary between satellite pairs within a plane and between planes. The actual behavior varies from case to case. However, the variations are periodic in the range of $\pm y_M$. Therefore, on average, variations and the total corresponding ΔV should be estimated conservatively.

To summarize the model, a) it is trained to estimate AOL relative in- and inter-plane drift rates between satellite pairs with Equation 2 and with features given by Equation 5; b) nine inclination groups are used resulting in nine sets of $\Theta(i)$; c) for equatorial orbits, a simple linear model is used given by Equation 6, and d) drift rates for different satellite/plain pairs are distributed between plus-minus maximum drift rates given by Equations 7 and 8.

Training the drift estimation model

In order to train the model and characterize the drift rates, we use Monte Carlo batch simulations in GMAT, with initial conditions within ranges of orbital elements presented in Introduction. Only JGM-2 gravitational perturbations are enabled and Brouwer–Lyddane long-term averaged mean elements are used to calculate relative AOL drift rates. Since orbits are near circular, the AOL is calculated as a sum of the AOP and the MA.

Equation 2 is solved using y_M with inclination i groups given in the previous subsection. For groups 0°–6° and 174°–180°, we used features given by Equation 6. For other groups, features given by Equation 5 are used. The training was performed on 8077 simulation results. Each simulation has 72 satellites which results in 2556 combinations of satellite pairs. Their initial TA separation ranges from 5° to 180° with 5° steps. For training, we use maximum drift rates y_M^u after five days in each TA separation group.

The outcome of training are $\Theta(i)$ coefficients, given in Appendix A.

We present some of the worst cases (i.e., includes underestimations of the maximum drift rate) from three simulations, as compared with predictions using Equation 4. Here, the model has been applied on the same data set which was used for training. The next subsection presents validation of the model with an independent data set. Mid-inclination, polar and equatorial cases are presented in Figure 1. Blue circles represent the drift between every pair of 72 satellites under J_2 over five days. The period of five days has been used to generate the training data set. As Equations 7 and 8 show, drift rates can be extrapolated for longer periods. The orange line represents an estimation of the largest drift in each TA separation group. The periodicity is not included in the estimation since we are not emulating a constellation yet but rather characterizing the model.

For TAT-C, the goal is to estimate the total ΔV required to maintain a topology. Therefore, we are more interested in the total maintenance resources as opposed to specific satellite pairs presented in Figure 1. For example, while the drift between satellites in different orbital planes has a large variation, the model captures the average upper bound quite accurately. Figure 2 shows the average drift rates for the AOL as simulated under J_2 and as predicted by the model using the

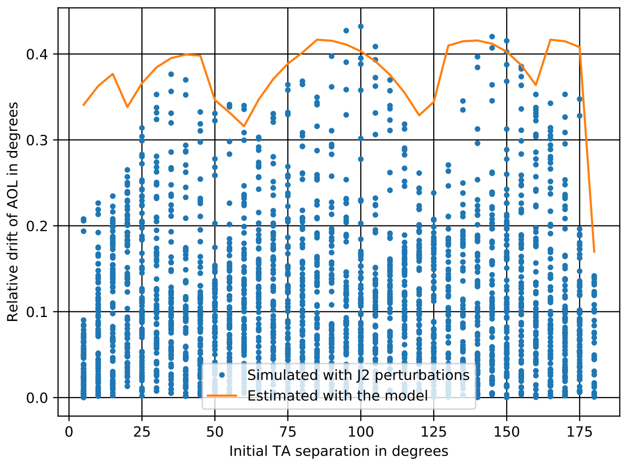

(a) Inclination of 36° and altitude of 378 km. Twelve orbital planes with six satellites per plane.

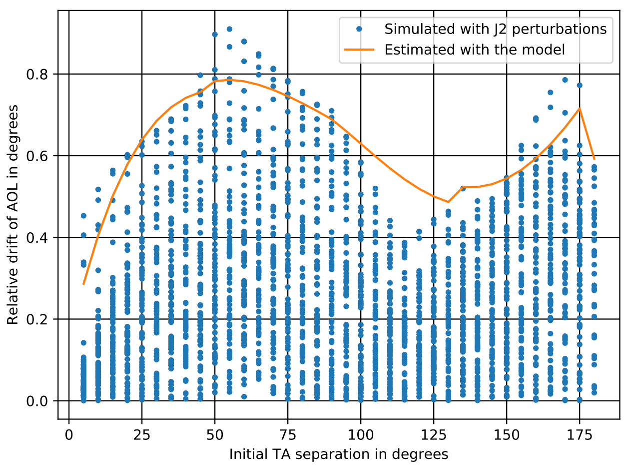

(b) Inclination of 88° and altitude of 419 km. Nine orbital planes with four satellites per plane.

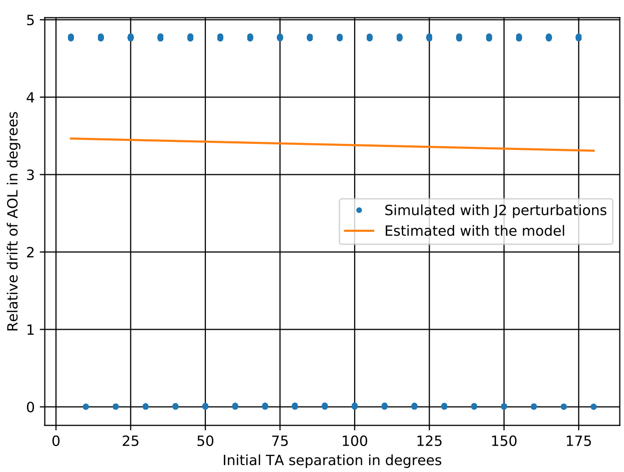

(c) Inclination of 0.3° and altitude of 614 km. Two orbital planes with 36 satellites per plane.

Figure 1: The AOL drift rate for all pairs of 72 satellites, as a function of the the initial TA separation, under J_2 perturbations (blue circles), and an estimate of the largest AOL drift rates from our proposed model (orange line).

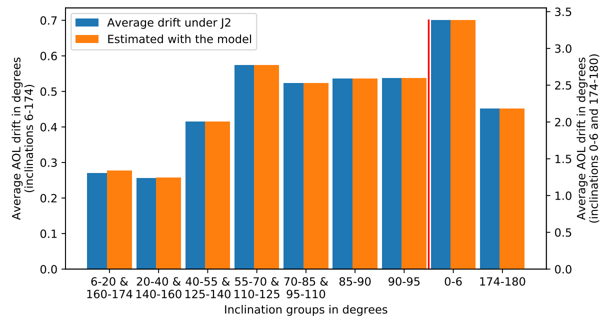

Figure 2: Average AOL drift rates due to J_2 and as predicted by the model over five days. The training data set is used here.

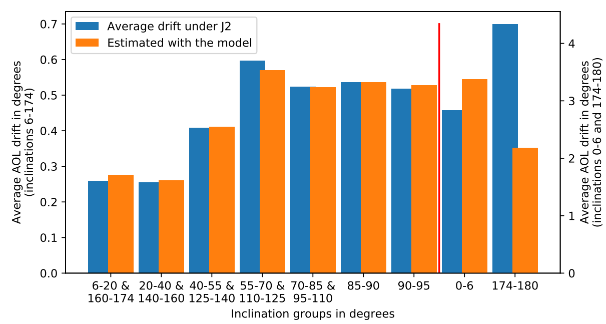

Figure 3: Average AOL drift rates due to J_2 and as predicted by the model over five days. The validation data set is used here.

training data set. Owing to our large training data, on average, there are no noticeable differences between the simulated J_2 drift rates and the modelled ones.

Validating the drift estimation model

In order to validate the model, an independent data set of 2000 simulations is used. Figure 3 shows the average drift rates for the AOL as simulated under J_2 and as predicted by the model using the validation data set. For nearly all inclination groups, the model predicts the AOL drift rates under J_2 fairly well. The model works less well for equatorial orbits by overestimating drift rates in the inclination group of 0°–6° and underestimating for 174°–180°. This suggests that the same model is not suitable for both inclination groups, and their training can be partitioned for future research. Note that equatorial orbits are seldom used for EO and the drift rate of almost 1° per day suggests that stationkeeping is expensive.

3. Atmospheric drag

Deorbiting model

The deorbiting rate due to the atmospheric drag in near circular orbits can be estimated using Eq. 9 [6, p. 215].

$$\Delta a_{rev} = -2\pi \left(\frac{C_d A}{m} \right) \rho a^2 \qquad (9)$$

Δa_{rev} is the change in the SMA per revolution.

C_d is the drag coefficient.

A is the is the satellite's cross-sectional area.

m is satellite's mass.

a is the initial SMA.

ρ is the atmospheric density.

For missions whose lifetimes are multiple years and altitudes are larger than 300 km, we model the atmospheric density depending on the 11-year solar cycle and ignore variations with smaller periods, such as the day–night and semi-annual cycles. Nevertheless, predicting the atmospheric density is a daunting task due to the irregular behavior of the solar activity. However, TAT-C, as its name suggests, is a tool for exploring tradespaces and, therefore, it is sufficient to estimate the total ΔV budget with a safety margin. We use a simple analytical representation of the atmospheric density which is given in Equation 10 [7, p. 246].

$$\rho = \rho_m + (\rho_M - \rho_m) sin^4(\frac{\pi t_s}{P}) \tag{10}$$

ρ is the atmospheric density at a given time during the solar cycle.

ρ_m is the density at a given altitude during the solar minimum.

ρ_M is the density at a given altitude during the solar maximum. We use a lookup table to find ρ_m and ρ_M for a specific altitude [6, p. 1031]. Since the table provides densities for altitudes with 50- or 100-km step sizes, linear interpolation is used to find a density at a given altitude.

P is the period of a solar cycle. While the period is ≈11 years, it varies from cycle to cycle, and the beginning is usually not well defined. Defining $\frac{P}{2}$ such that it coincides with the solar maximum will provide the most reliable results.

t_s is the time measured from the solar minimum.

Validating the deorbiting model

We validate the model by propagating a satellite for 100 days, starting at various epochs (satellites deployed at different absolute start dates) under the atmospheric drag. We compare deorbiting rates with the ones predicted by Equation 9. Figure 4 shows results from the comparison. Blue circles show propagation with the Jacchia–Roberts atmospheric model and the orange line shows estimation with the model presented above. The reference for the relative epoch is November 1, 1995 which approximately coincides with the beginning of the last full solar cycle. The solar-cycle period is set to 10.5 years which is not strictly correct but helps to align $\frac{P}{2}$ with the solar maximum. The rapid deorbiting rate on the absolute scale is because we selected a three-unit CubeSat with a mass of 3.8 kg, the drag coefficient of 2.2 and the satellite's cross-sectional area of 0.1156 m^2, as a pessimistic estimate for deorbiting validation. As expected, the model presents the general trend that

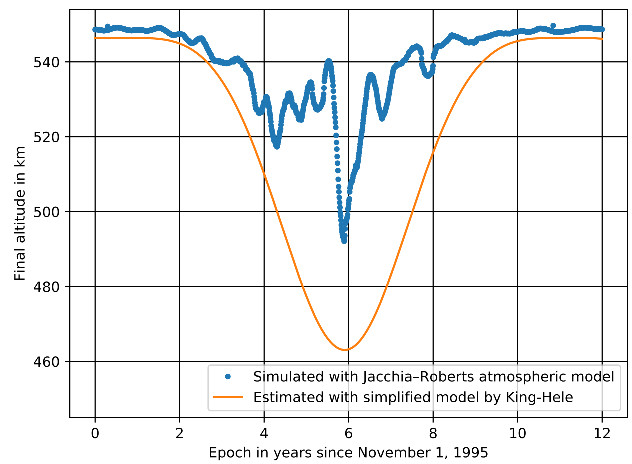

Figure 4: Loss of spacecraft altitude as a function of its deployment epoch/time, as evaluated by orbit propagation on GMAT with the Jacchia–Roberts atmospheric model (blue circles), and by the model proposed for TAT-C's OMM (orange line). Each blue circle presents the final altitude after 100 days starting from 550-km altitude. For each consecutive simulation, the epoch is increased by three days.

the deorbiting rate increases as the epoch approaches the solar maximum which takes place right before the relative epoch of six years. It provides the worst-case scenario for deorbiting rates which is desirable for TAT-C.

4. Orbit maintenance

The OMM of TAT-C uses user-defined inputs in computing orbital degradation per the presented models, followed by orbital maneuvers, propellant accounting and other output metrics, per user-defined requirements, for further tradespace analysis. Figure 5 summarizes the information flow within the OMM. A mission is advanced by iteratively stepping through time since the epoch of a mission until its lifetime is breached. Every orbit, the change in altitude is calculated. Every day (or a customizable time step), the relative drift in AOL is recalculated and the atmospheric density is updated. When drift rates breach the user-defined thresholds, the next time step/s is allocated for performing maneuvers. The timeline of maintenance, including the maneuver type, satellite/plane index and ΔV, is saved along with the mass of leftover propellant of each satellite.

Constellation architectures

The current version of TAT-C explores a tradespace of constellation architectures, where the satellites have the same dry mass, drag coefficient and area, as well as the same initial propellant mass. The homogeneous Walker, train and precessing-type (upon stabilization) architectures place all satellites in orbits with equal initial altitudes and inclinations [8]. The satellites in heterogeneous Walker and ad-hoc constellations experience large relative drifts among the satellites because their orbits have different altitudes and/or inclinations. The presented models of in-plane maintenance may be

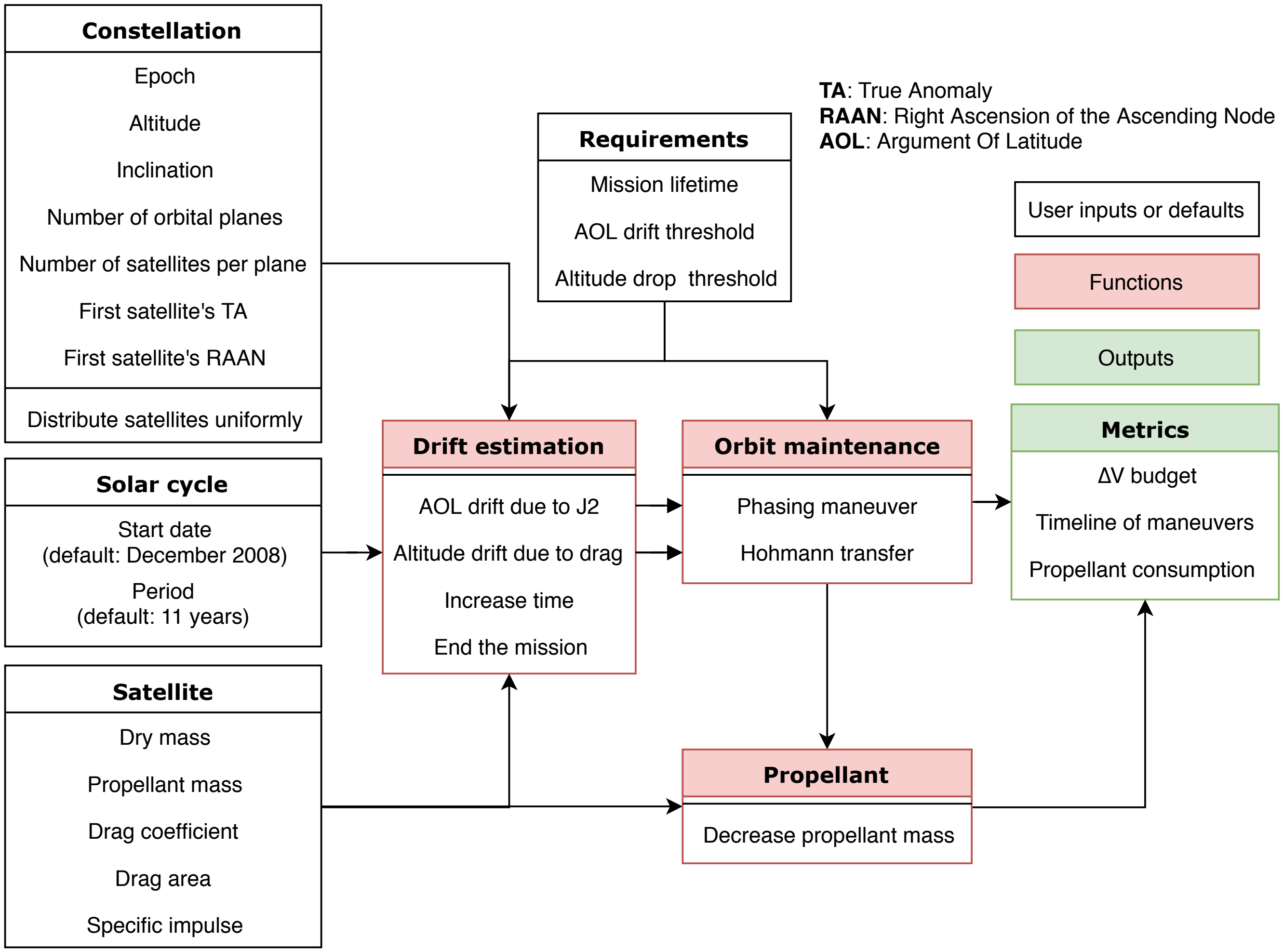

Figure 5: Information flowchart for the Orbit Maintenance Module.

used to compute metrics for heterogeneous Walker, but from an inter-plane perspective, such constellations are characterized by their constantly changing topologies. For the purpose of presenting OMM's results in this paper, a homogeneous Walker constellation is defined by its altitude, inclination the number of orbital planes and the number of satellites per plane. Since they are distributed uniformly according to the Walker-Delta pattern, only the first satellite's TA and RAAN are required as inputs. The user can also chose to replace default solar cycle parameters – the start date and the period. All orbits are assumed circular.

Orbital maneuvers

To correct for the drifting relative AOL and altitude, we use simple orbital maneuvers of orbit phasing [5, p. 362] and Hohmann transfer [6, p. 226], respectively. Single impulse of chemical propulsive maneuvers are currently modeled, however, the OMM may be expanded to include electric propulsion in the future. The relative AOL drift is compensated by each satellite emulating a phasing maneuver equal to a half of the relative drift between one out of two neighbors. For example, the first satellite compensates a half of the drift between the first and the second satellite. Since orbits are not propagated, the maneuvers are used to calculate the required ΔV and corresponding elements are just reset to their nominal values. When a pair of satellites within a plane breach a threshold, orbital maneuvers are emulated for all satellites in the plane. Note that relative corrections between a pair of satellites possibly automatically alleviates or worsens the relative error between one of them with respect to a third, since all satellites are arranged in a homogenous circle. A similar approach is taken with the inter-plane AOL drift – as soon as the threshold is breached between satellites in two planes, the relative drift is corrected for satellites in all planes. Such an approach simplifies the code, provides the same average ΔV estimates and also keeps the relative differences in elements to a minimum which, in turn, minimizes the future relative drift. The propellant mass is decreased by calculating the impulse using ΔV from emulated maneuvers and then using the given specific impulse of the propulsion system.

Validating the Orbit Maintenance Module

We validate the OMM of TAT-C by running GMAT simulations that the OMM attempts to emulate without running orbital perturbations, and comparing them to the OMMs results, for two use cases – CYGNSS (Cyclone Global Navigation Satellite System) and TROPICS (Time-Resolved Observations of Precipitation structure and storm Intensity with a Constellation of Smallsats). OMM's results capture the automation of maintaining any given constellation – estimation of orbital degradation, orbital maneuver computation, and the resultant corrected orbits. First, a single orbital plane case of a constellation similar to CYGNSS is validated. The following satellite, orbital and constellation parameters are used to set up the GMAT simulation and the OMM [10].

- J_2 and atmosphere models enabled.
- The satellite mass of 27.5 kg with additional 7 kg for the propulsion system and propellant, since the original design does not include a propulsion system.
- Eight satellites distributed uniformly in a single orbit. The initial TA separation is 45°.
- Constellation altitude of 525 km.
- Constellation inclination of 35°.
- The first satellite's (sat0) TA of 207°.
- The first satellite's RAAN of 144°.
- Drag coefficient of 2 with the drag area of 0.1428 m^2.
- Specific impulse of 230 s.
- Initialization epoch on December 15, 2016 at 13:37 UTC.
- AOL drift threshold of 0.5% (0.225°).
- Altitude drop threshold of 0.1% (0.525 km).
- Although the mission lifetime is two years, we simulate 31 days because the drift cycles and corresponding maneuvers are periodic.

The phasing maneuvers within the GMAT comparison scenario are performed slightly differently than those by the OMM, however the effect on constellation topology or maintenance metrics remains minor. In GMAT, the first satellite is used as a reference for the AOL and each sequential satellite is maneuvered to an AOL with 45° steps. Such an approach requires slightly less propellant than correcting for a half of the relative AOL drift. This, in turn, overestimates the propellant budget which is desirable for TAT-C.

Figure 6 shows the relative AOL between eight satellites in a CYGNSS-like constellation, as simulated by GMAT. It takes nearly five days for the relative AOL between sat3 and sat4 to breach the 0.225° threshold. An automated sub-function in GMAT performs the maneuvers satellite by satellite. With the exception that it takes more time, the effect is the same as maneuvering all satellites simultaneously but GMAT does not provide such functionality. A satellite is propagated to the perigee where the first phasing maneuver is performed following the second maneuver after an orbit. While the maneuver sub-function is executed, the AOL values are not reported and, therefore, the relative AOLs remain constant. When all satellites have performed their phasing maneuvers, GMAT returns to the main sequence which reports the relative AOLs. They are not nullified entirely because the satellites continue to drift during the maneuver phase. Over 31 days, the relative AOL drift is compensated six times.

Figure 7 shows the altitude drop of the CYGNSS constellation, as simulated by GMAT. During the 31-day period, the altitude threshold is breached and compensated once around day 22. A Hohmann transfer is performed by propagating the satellite to the perigee, where apogee-raising maneuver is performed, and then to the apogee where the circularization burn is performed.

Table 1 summarizes all maneuvers along with the time when a threshold was breached and the total mass of propellant required to perform maneuvers, and represents the GMAT simulation results that the OMM results are compared against. Phasing maneuvers correct for drifts due to gravitational perturbations, while Hohmann maneuvers correct for altitude drop due to the atmospheric drag. Each set of phasing maneuvers requires ≈0.11 kg of propellant and the Hohmann transfer – 0.0323 kg. Table 2 summarizes the results of the OMM which emulated the CYGNSS constellation with the same parameters. The phasing maneuvers are only slightly more expensive requiring >0.13 kg per set of maneuvers. The propellant required for the Hohmann transfer is nearly the same for both approaches, validating OMMs proposed corrections. The most noticeable difference is the number of phasing maneuvers. In GMAT, the relative AOL drifts faster than in the OMM resulting in six versus five maneuvers. Nevertheless, the OMM

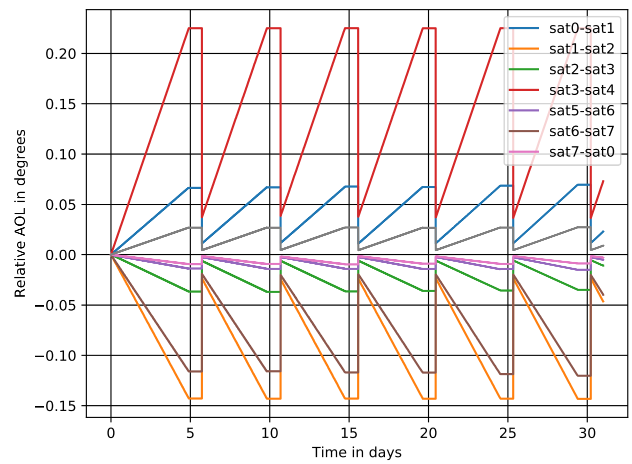

Figure 6: GMAT simulation results: The relative AOL drift between eight consecutive satellites of the CYGNSS constellation, and phasing maneuvers that correct for the drift when a 0.5% threshold is breached.

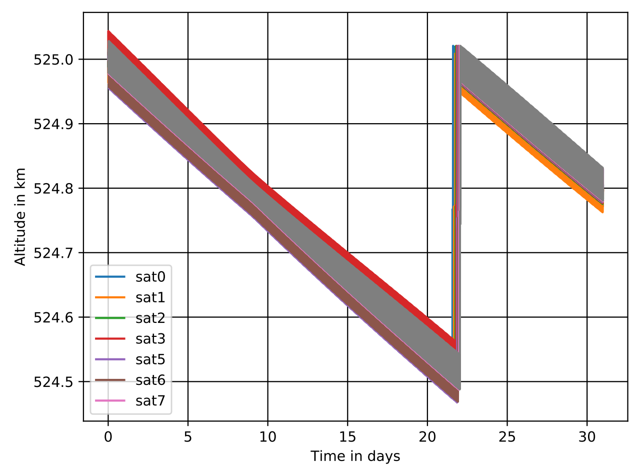

Figure 7: GMAT simulation results: The altitude drift of eight satellites of the CYGNSS constellation, and Hohmann transfers that raise orbits when a 0.1% threshold is breached.

budgets for slightly more propellant due to the designed overestimation when performing phasing maneuvers, therefore sufficiently compensates for this difference.

Table 1: GMAT simulation result to validate against TAT-C's OMM: A sequence of maneuvers and the required propellant.

Maneuver	Time (days)	Required propellant (kg)
Phasing	4.9	0.10986
Phasing	9.8	0.10978
Phasing	14.7	0.10998
Phasing	19.6	0.10991
Hohmann	21.5	0.03230
Phasing	24.5	0.11021
Phasing	29.4	0.11059
		Total: 0.693

Table 2: TAT-C OMM results: A sequence of maneuvers and the required propellant.

Maneuver	Time (days)	Required propellant (kg)
Phasing	5	0.13389
Phasing	11	0.13472
Phasing	17	0.13465
Hohmann	21	0.03536
Phasing	23	0.13449
Phasing	29	0.13266
		Total: 0.706

Second, we attempt to validate a case where satellites are placed in multiple orbits and experience the relative AOL inter-plane drift. The TROPICS constellation [11] was simulated with three orbital planes containing two satellites each. Figure 8 shows that the relative AOL inter-plane drift is not linear in the timescale of five days which was used in training the model. Therefore, the current OMM model largely overestimates the relative AOL inter-plane drift (i.e., a breach is predicted five times earlier than it takes place in GMAT), and needs a scaling correction. Data simulations within similar parameters as proposed in this paper, except with a longer timescale, are required to to train the model and improve its fidelity. The GMAT validation data in Figure 8 demonstrates that the AOL drift behavior across planes can be approximated by a linear fit, even if the shorter timespans are characterized by periodic oscillations. Corrections computed from linearized predictions will therefore be a sufficient pre-Phase A assumption for maintenance overhead for a multi-plane constellation.

5. Summary and future work

We have developed an Orbit Maintenance Module (OMM) for Tradespace Analysis Tool for Constellations (TAT-C). The module includes computationally-lightweight models which estimate the secular relative drift of orbital elements due to J_2 gravitational effects and the atmospheric drag.

The J_2, primarily, affects the Argument Of Latitude (AOL) which is a sum of the argument of perigee and the true anomaly. The maximum secular drift of the AOL is estimated by a fourth-order model with 20 features. It depends on the initial separation in the true anomaly and in the right ascension of the ascending node, as well as

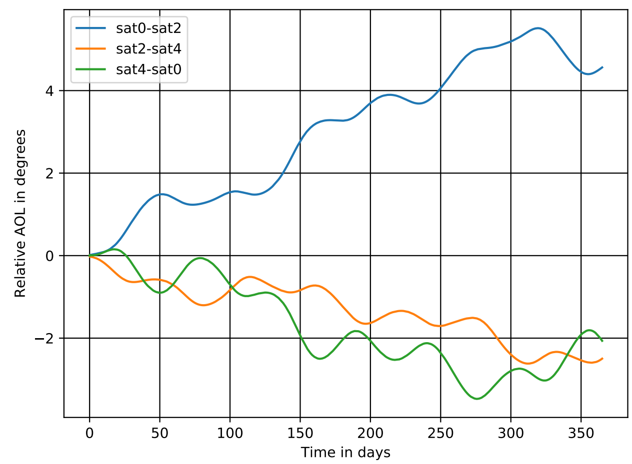

Figure 8: GMAT simulation results: The relative AOL drift between satellites in the three orbital planes of the TROPICS constellation.

on the altitude and the inclination. The normal equation was used to train the model with a data set generated using Monte Carlo simulations in GMAT. Coefficients were found for each affected element in nine inclination groups. When emulating a constellation drift rates are assigned within the range of plus-minus the maximum modeled drift.

The deorbiting rate is estimated using a pre-existing analytical model which depends on the atmospheric density. We account for the 11-year solar cycle using a very rough-and-ready model. The model ignores short-term variations within the cycle which ultimately depend on fairly unpredictable sunspots. Nevertheless, we validated that both models combined can predict the general deorbiting trend and set an upper limit for the deorbiting rate. Orbital maneuvers of Hohmann transfer and orbit phasing are emulated to estimate the needed ΔV and the corresponding propellant consumption when drift rates breach a given threshold.

The OMM has been validated against a single orbital plane case of CYGNSS simulations in GMAT. The OMM underestimated the relative AOL drift rate by $\approx$10% which was compensated by a $\approx$20% overestimate in propellant consumption resulting in a slight overall overestimate (<2%) in the total propellant consumption. The altitude drift rate and propellant consumption were estimated within 10%, therefore the 5-day dataset and subsequently trained model was validated to be appropriated for in-plane and altitude drifts. In the three orbital plane case of TROPICS, the relative inter-plane AOL drift turned out to be non-linear rendering the OMM model, which was trained on five-day data sets, largely overestimating the drift rate. Therefore, the future work includes the following.

- Development of a model which is trained on timescales of several months for the relative AOL inter-plane drift.
- Validation against a larger set of high-fidelity constellation simulations.

Setting up a constellation in the orbit maintenance module takes $\sim$1 minute if the orbital elements and satellite parameters are known. Setting up a constellation in GMAT can a take time between an hour to a day, depending on the size of a constellation and the user's experience. Running a multi-year mission in the OMM takes several seconds on a modest laptop while a GMAT simulation can take a couple of hours. A short set-up time and fast execution are the main benefits of the pre-Phase A analysis in TAT-C to get reliable estimates for orbit maintenance.

Acknowledgments

This research is supported by the project "Generalizing Distributed Missions Design Using the Trade-Space Analysis Tool for Constellations and Machine Learning" (NASA Grant Number: 80NSSC17K0572). The travel to the conference was supported by the University of Tartu ASTRA project 2014-2020.4.01.16-0029 KOMEET "Benefits for Estonian Society from Space Research and Application", financed by the EU European Regional Development Fund.

References

[1] J. Le Moigne, P. Dabney, O. de Weck, V. Foreman, P. Grogan, M. Holland, S. Hughes, and S. Nag, "Tradespace analysis tool for designing constellations (TAT-C)," in *IEEE International Geoscience and Remote Sensing Symposium (IGARSS)*. IEEE, 7 2017, pp. 1181–1184. [Online]. Available: http://ieeexplore.ieee.org/document/8127168/

[2] S. Nag, S. P. Hughes, and J. Le Moigne, "Streamlining the Design Tradespace for Earth Imaging Constellations," in *AIAA SPACE*. Reston, Virginia: American Institute of Aeronautics and Astronautics, 9 2016. [Online]. Available: http://arc.aiaa.org/doi/10.2514/6.2016-5561

[3] D. G. King-Hele, G. E. Cook, and H. M. Watson, "Even Zonal Harmonics in the Earth's Gravitational Potential," *Nature*, vol. 202, no. 4936, pp. 996–996, 6 1964. [Online]. Available: http://www.nature.com/doifinder/10.1038/202996a0

[4] K. T. Alfriend, *Spacecraft formation flying : dynamics, control and navigation*. Elsevier/Butterworth-Heinemann, 2010.

[5] D. A. Vallado and W. D. McClain, *Fundamentals of astrodynamics and applications*, 4th ed. Microcosm Press, 2013.

[6] J. R. Wertz, D. F. Everett, and J. J. Puschell, *Space Mission Engineering: The New SMAD*. Microcosm Press, 2011.

[7] D. King-Hele, *Satellite orbits in an atmosphere: Theory and applications*. Blackie, 1987.

[8] S. Nag, S. P. Hughes, and J. J. Lemoigne, "Navigating the Deployment and Downlink Tradespace for Earth Imaging Constellations," in *68th International Astronautical Congress (IAC)*, Adelaide, Australia, 2017.

[9] Andrew Ng, "Machine Learning on Coursera." [Online]. Available: https://www.coursera.org/learn/machine-learning

[10] T. Finley, D. Rose, K. Nave, W. Wells, J. Redfern, R. Rose, and C. Ruf, "Techniques for leo constellation deployment and phasing utilizing differential aerodynamic drag," in *Advances in the Astronautical Sciences*, 2014.

[11] W. J. Blackwell, S. Braun, R. Bennartz, C. Velden, M. DeMaria, R. Atlas, J. Dunion, F. Marks, R. Rogers, B. Annane, and R. V. Leslie, "An overview of the TROPICS NASA Earth Venture Mission," *Quarterly Journal of the Royal Meteorological Society*, 2018.

Biography

Dr. Andris Slavinskis *was a Research Scientist at NASA Ames Research Center (contracted by Bay Area Environmental Research Institute). Currently, he is a Postdoc at Aalto University and a Senior Researcher at Tartu Observatory, University of Tartu, Estonia. He received BSc and MSc degrees in computer science from Ventspils University College, Latvia in 2009 and 2011, as well as a PhD in physics from the University of Tartu in 2015. Slavinskis is interested in nanosatellites, nanospacecraft, and multi-satellite mission designs. He has received IEEE "Harry Rowe Mimno Award" 2016.*

Dr. Sreeja Nag *is a Senior Research Scientist at NASA Goddard Space Flight Center and NASA Ames Research Center (contracted by Bay Area Environmental Research Institute). She completed her PhD in Space Systems Engineering from the Department of Aeronautics and Astronautics at Massachusetts Institute of Technology. Her research interests include distributed space systems, automated planning and scheduling of constellations, swarm decision making in space, and space traffic management.*

Joel Mueting *is a flight dynamics engineer at NASA Ames Research Center. He completed his B.S. in Aerospace Engineering in 2014 and M.S. in Systems Engineering in 2016 at the University of Arizona. His research interests include expanding the capability of small satellites through distributed space systems and formation flight.*

Appendices

A. $\Theta(i)$ coefficients

$\Theta(6° \ldots 20° \bigcup 160° \ldots 174°) =$

[5.46e-01, 1.11e-03, -1.76e-05, 4.74e-03, -1.77e-05, -3.74e-02, 2.08e-04, -1.48e-04, -3.26e-05, 1.68e-07, 1.28e-07, -6.35e-10, 1.73e-04, -7.35e-07, -9.67e-07, 4.11e-09, -3.11e-08, 2.09e-10, 9.62e-08, -2.30e-10]

$\Theta(20° \ldots 40° \bigcup 140° \ldots 160°) =$

[-3.08e-01, 5.11e-03, -2.72e-05, 4.22e-03, -1.71e-05, 1.58e-02, -8.75e-05, -1.19e-04, -6.07e-05, 3.19e-07, 2.18e-07, -1.09e-09, 2.02e-05, -1.88e-07, -1.23e-07, 1.09e-09, -8.60e-07, 4.17e-09, 1.45e-08, 2.20e-11]

$\Theta(40° \ldots 55° \bigcup 125° \ldots 140°) =$

[-5.01e-01, 1.31e-02, -1.19e-04, 6.19e-03, -2.48e-05, 1.77e-02, -9.80e-05, -2.13e-04, -7.60e-05, 3.86e-07, 2.46e-07, -1.14e-09, -7.25e-06, -6.31e-08, 1.41e-08, 4.83e-10, -8.20e-07, 4.89e-09, 3.19e-07, -4.24e-11]

$\Theta(55° \ldots 70° \bigcup 110° \ldots 125°) =$

[7.68e-01, 1.91e-02, -3.38e-04, 3.99e-03, -1.79e-05, -1.10e-02, 5.56e-05, -3.41e-04, -1.08e-04, 6.01e-07, 5.01e-07, -2.79e-09, 2.24e-04, -1.21e-06, -1.28e-06, 6.91e-09, -1.23e-06, 6.41e-09, 1.95e-06, -3.29e-09]

$\Theta(70° \ldots 85° \bigcup 95° \ldots 110°) =$

[-2.97e-01, 1.33e-02, -3.77e-04, 4.06e-03, -1.37e-05, 6.93e-03, -3.98e-05, -2.63e-04, -7.58e-05, 3.95e-07, 2.22e-07, -1.16e-09, 5.11e-04, -2.65e-06, -2.84e-06, 1.48e-08, -2.18e-06, 1.24e-08, 2.55e-06, -4.50e-09]

$\Theta(85° \ldots 90°) =$

[-5.00e+00, -5.68e-02, 4.72e-05, 3.03e-03, -7.74e-06, 1.12e-01, -6.33e-04, -2.66e-04, -6.48e-05, 3.24e-07, 1.12e-07, -5.37e-10, 2.27e-03, -1.45e-05, -1.31e-05, 8.37e-08, -2.81e-06, 1.59e-08, 3.07e-06, -5.47e-09]

$\Theta(90° \ldots 95°) =$

[6.90e+00, -1.64e-01, 4.18e-04, 2.97e-03, -7.22e-06, -1.47e-01, 7.80e-04, -2.67e-04, -6.48e-05, 3.13e-07, 1.26e-07, -5.27e-10, 4.44e-03, -2.17e-05, -2.39e-05, 1.17e-07, -3.01e-06, 1.69e-08, 3.08e-06, -5.50e-09]

$\Theta(0° \ldots 6°) =$ [3.47e+00, -1.48e-06]

$\Theta(174° \ldots 180°) =$ [2.37e+00, -3.01e-06]